The human immune checkpoint molecule, HLA-G2, induces tolerance in monocytes and dendritic cells via upregulation of PD-L1

Immunosuppressive effects of HLA-G2 on monocytic cells

Authors:

Ami Takahashi[1], Kimiko Kuroki[1,*], Naoyoshi Maeda[2,3], Mie Nieda[4], Katsumi Maenaka[1,2,5,6,7,*]

Author affiliations:

[1]Laboratory of Biomolecular Science, Faculty of Pharmaceutical Sciences, Hokkaido University, Kita-12, Nishi-6, Kita-ku, Sapporo 060-0812, Japan

[2]Center for Research and Education on Drug Discovery, Faculty of Pharmaceutical Sciences, Hokkaido University, Kita-12, Nishi-6, Kita-ku, Sapporo 060-0812, Japan

[3]School of Pharmaceutical Sciences, Health Sciences University of Hokkaido, 1757 Kanazawa, Tobetsu-cho, Ishikari-gun, Hokkaido 061-0293, Japan

[4]Biotherapy Institute of Japan Ltd. 2-4-8 Edagawa, Koto-ku, Tokyo, 135-0051 Japan.

[5]Institute for Vaccine Research and Development (HU-IVReD), Hokkaido University; Sapporo, Japan

[6]Global Station for Biosurfaces and Drug Discovery, Hokkaido University, Sapporo,

Japan

[7]Faculty of Pharmaceutical Sciences, Kyushu University, Fukuoka, Japan

***Corresponding authors:**

k-kimiko@pharm.hokudai.ac.jp (K. Kuroki), maenaka@pharm.hokudai.ac.jp (K. Maenaka)

Classifications:

BIOLOGICAL SCIENCES, Immunology and Inflammation

Keywords:

LILRB2, HLA-G2, PD-L1, tolerance, immune checkpoint receptor

The authors declared no conflict of interest. A.T., K.K. and K.Maenaka have filed an application with Japanese patent office.

Abstract

Human leukocyte antigen (HLA)-G is a non-classical HLA class I immunomodulatory molecule with restricted expression in the placenta, thymus and regulatory T cells. The spliced isoforms of HLA-G include an α2 domain-deleted isoform, HLA-G2, which specifically binds to the immune checkpoint leukocyte immunoglobulin-like receptor B2 (LILRB2), to suppress immune responses in myelomonocytic cells. We previously reported the structural and receptor binding characteristics of recombinant HLA-G2 protein and its immunosuppressive effects on inflammation in mouse models. However, the function and the mechanism of action of HLA-G2 on human immune cells have not been elucidated.

In the present study, we demonstrate the immunosuppressive effect of HLA-G2 on human CD14-positive monocytic cells. HLA-G2 induced the production of the immunosuppressive cytokine, IL-10, and stimulated IL-6/STAT3/indoleamine-2,3-dioxygenase signaling by binding to LILRB2. HLA-G2 binding to LILRB2 also down-regulated cell surface expression of HLA-DR and CD86. Unexpectedly, HLA-G2 up-regulated cell surface expression of PD-L1 in both CD14-positive monocytic cells and interferon-induced dendritic cells (IFN-DCs). This observation suggests HLA-G2/LILRB2 signaling promotes PD-L1 expression. Furthermore, HLA-G2 treatment of IFN-DCs suppressed T cell proliferation in mixed lymphocyte reactions. These findings provide novel insights into the modulation of human immune responses of tolerogenic

58 myelomonocytic cells induced by HLA-G2 binding to LILRB2, and suggest that targeting
59 the HLA-G2-LILRB2 interaction could be a novel approach for immune checkpoint
60 therapy.
61

62 **Significance statement**

63 During pregnancy, HLA-G isoforms are expressed by fetal trophoblasts to suppress
64 maternal immune responses. Among various HLA-G isoforms, the HLA-G2 homodimer
65 has been expected as an immunosuppressive biologic targeting myelomonocytic antigen-
66 presenting cells via leukocyte immunoglobulin-like receptor B2. We previously reported
67 significant immunosuppressive effects of HLA-G2 in autoimmune mouse models. Here,
68 we first demonstrate that HLA-G2 isoform induces tolerogenic phenotypes of human
69 peripheral immune cells by significantly upregulating an immune checkpoint molecule,
70 PD-L1. Monocyte-derived dendritic cells stimulated by HLA-G2 suppressed T cell
71 proliferation in mixed lymphocyte reactions. These results suggest that HLA-G2 can be
72 a novel candidate for immune checkpoint therapy.

73

74

75

76 **Introduction**

77 Human leukocyte antigen-G (HLA-G) plays an important role in immune tolerance. The
78 characteristics of HLA-G are distinct from classical HLA class I molecules: low
79 polymorphism, restricted tissue distribution, and expression as several spliced isoforms
80 (1-3). The restricted expression of HLA-G on placental trophoblasts contributes to
81 maternal-fetal immune tolerance (4). HLA-G is also expressed in thymic tissue (5) and
82 regulatory T cells (6). HLA-G expression is also observed in pathological conditions such
83 as tumorigenesis, viral infections, and transplantation (7). To date, seven spliced isoforms
84 of HLA-G have been reported. HLA-G1 to HLA-G4 are membrane-bound isoforms and
85 HLA-G5 to HLA-G7 are soluble isoforms (1-3) (Supplementary Figure 1). HLA-G1 and
86 HLA-G5, which have identical extracellular domains, share a similar structural
87 organization to classical HLA class I molecules composed of a heavy chain (α1, α2 and
88 α3 domains), a peptide, and β2-microgrobulin (β2m). By contrast, HLA-G2 and HLA-
89 G6, which have identical extracellular domains, form a non-covalently linked homodimer
90 of two α2 domain-deleted heavy chains (α1 and α3 domains), which structurally
91 resembles the heterodimer of HLA class II molecules (8).

92 HLA-G isoforms inhibit immune responses by binding the inhibitory leukocyte
93 immunoglobulin (Ig)-like receptors (LILR) B1 and LILRB2. LILRB1 and LILRB2
94 transmit inhibitory signals to immune cells by binding broadly to classical and non-
95 classical HLA class I molecule under physiological conditions. The binding affinity of

96 HLA-G1 to LILRB receptors is higher than other HLA class I molecules (9). LILRB1 is
97 expressed on a broad range of immune cells such as antigen presenting cells (APCs), T
98 cells and natural killer (NK) cells. By contrast, LILRB2 is mainly expressed on
99 myelomonocytic cells, including monocytes, macrophages, and dendritic cells (DCs) (10).
100 A mouse orthologue of human LILRB2, the paired Ig-like receptor (PIR)-B, is expressed
101 on APCs and binds to both HLA-G1 and HLA-G2 (11, 12). Both HLA-G1 and HLA-G2
102 promote the immunosuppression in inflammatory disease mouse models (11-16).
103 The immunosuppressive mechanism of HLA-G1 has been widely studied. HLA-G1
104 binding to LILRB1 broadly inhibits immune cell function, such as proliferation and
105 differentiation of T and B cells, and Ig secretion (17, 18). In addition, HLA-G1 inhibits
106 DC maturation in part by downregulating HLA class II, CD80, and CD86, and prolongs
107 the allograft survival (19, 20). HLA-G1 binding to LILRB2 modulates the IL-6 signaling
108 pathway and STAT3 activation in LILRB2 transgenic mice and human monocyte-derived
109 DCs (19, 21). In human macrophages, soluble HLA-G1 increases IL-6 and indoleamine-
110 2,3-dioxygenase 1 (IDO-1) production, which inhibits T cell activation (22). By contrast
111 to HLA-G1, the function and mechanism of action of the HLA-G2 isoform remains
112 unclear.
113 Individuals homozygous for the *HLA-G*0105N* allele do not express the functional
114 HLA-G1 isoform but can still produce α2 domain-deleted HLA-G2 and HLA-G6
115 isoforms. Interestingly, HLA-G2 bound to LILRB2 with high affinity by avidity effect

116 (8). Furthermore, the soluble HLA-G2 protein showed anti-inflammatory effects in a
117 rheumatoid arthritis (RA) mouse model at lower doses compared to HLA-G1 monomers
118 and homodimers (11, 12). These observations clearly support the functional significance
119 of HLA-G2 in immune suppression *in vivo*. However, the effects of HLA-G2 on signaling
120 in human cells have not been defined.

121 In this study, we investigated the functional effect of HLA-G2 on human LILRB2-
122 expressing CD14-positive monocytes and monocyte-derived dendritic cells. HLA-G2
123 binding induced an immunosuppressive phenotype in monocytes, eliciting upregulation
124 of two key immunosuppressive molecules programmed death-ligand 1 (PD-L1) and IDO.
125 HLA-G2-treated DCs differentiated from peripheral blood monocytes with GM-CSF and
126 IFN-γ, designated as IFN-DCs (23), also showed an immunosuppressive phenotype and
127 inhibited proliferation of both CD4-positive and CD8-positive T cells in allogeneic and
128 autologous mixed lymphocyte reactions (MLR), respectively. This study provides a novel
129 insight into the mechanism of the immunosuppressive effects of the unique HLA-G
130 isoform, HLA-G2. Furthermore, it also suggests that targeting HLA-G2−LILRB2
131 signaling could provide a novel therapeutic intervention in diverse immune disorders.

132 **Materials and methods**

133 **Preparation of the recombinant HLA-G2 protein**

134 The extracellular domains of HLA-G2 (HLA-G2) were expressed in *Escherichia coli*
135 ClearColi BL21(DE3) competent cells (Lucigen) to avoid triggering endotoxic responses
136 in human cells. The inclusion bodies of HLA-G2 were refolded as previously described
137 (12). Refolded HLA-G2 protein was purified by size exclusion chromatography using
138 HiLoad 26/60 Superdex75 pg column (GE Healthcare) equilibrated with 20 mM Tris-
139 HCl pH 8.0, 100 mM NaCl. The peak of properly refolded HLA-G2 was collected and
140 buffer exchanged into HBS-EP (0.01 M HEPES pH 7.4, 0.15 M NaCl, 3 mM EDTA and
141 0.005% [v/v] Surfactant P20, GE Healthcare) for surface plasmon resonance (SPR)
142 analysis or PBS for cell-based assays by dialysis. HLA-G2 proteins in PBS were
143 concentrated by Amicon Ultra-15 (NMWL 10,000 Da) (Merck Millipore), and the
144 flowthrough solution from protein concentration was used as a negative control (PBS) in
145 cell-based assays. HLA-G2 and PBS solutions were filter sterilized through a 0.22 μm
146 filter.

147

148 **Preparation of human monocytes and DCs**

149 CD14-positive monocytes were isolated from peripheral blood mononuclear cells
150 (PBMCs) with CD14 microbeads and MACS LS column system (Miltenyi Biotec).
151 PBMCs were obtained from the buffy coats of twelve healthy blood donors (eight males

152 and four females, over twenty years old, Hokkaido University) by density gradient
153 centrifugation (Lymphoprep, Veritas) following the manufacturer's instructions. The
154 mean number of PBMCs and CD14-positive monocytes were 7.3 ± 1.5 x 10^7 cells/mL
155 and 8.2 ± 2.7 x 10^6 cells/mL, respectively. The average purity of CD14-positive
156 monocytes was calculated as 86 ± 7.0% by flow cytometry. CD14-positive cells were
157 incubated with 10% (v/v) HLA-G2 (final concentration of 2.3 μM) or 10% (v/v) PBS in
158 the culture medium (RPMI-1640 medium (Wako) containing 10%(v/v) heat-inactivated
159 FBS (Lot no. 10777, Biosera) and Penicillin-Streptomycin-Amphotericin B Suspension
160 (Wako)) at 37°C under 5% CO_2 condition either overnight or for two days (18 or 48 hours,
161 respectively). Cells cultured in medium alone were used as a non-treated control. CD14-
162 negative lymphocytes were collected for mixed lymphocyte reaction (MLR) assays.
163 IFN-DCs were differentiated from adherent PBMC cells in 10% FBS RPMI-1640
164 (Wako) or Gibco AIM V medium (Thermo Fisher Scientific) containing 1000 U/mL GM-
165 CSF (Primmune Inc.) and IFN-α (IFN-α 2b, OriGene Technologies or MSD) as
166 previously described (23). After three days, IFN-DCs were harvested, and cultured in
167 10% FBS RPMI-1640 or Gibco AIM V medium with 10% (v/v) HLA-G2 (final
168 concentration of 2.3 μM) or 10% (v/v) PBS for two days. Penicillin-Streptomycin-
169 Amphotericin B Suspension (Wako) were added in RPMI-1640 medium.
170 To generate immature IL-4-DCs, purified CD14-positive cells from PBMCs were
171 cultured in differentiation medium (10% FBS RPMI-1640 (Wako) with 1000 U/mL GM-

172 CSF (Primmune Inc.), 500 U/mL IL-4 (Primmune Inc.) and Penicillin-Streptomycin-
173 Amphotericin B Suspension (Wako)) for seven days.
174 The clinical study protocol was approved by the Bioethics Committee of Faculty of
175 Pharmaceutical Sciences, Hokkaido University (clinical research no. 2016-006).
176 Informed consents were obtained from all participating healthy donors prior to their
177 inclusion in this study.
178
179 **Flow cytometry (FCM) analysis**
180 Cells were harvested and suspended in 50 μL of FCM buffer (0.5% BSA and 0.05%
181 sodium azide in PBS) with 2.5-10 μg of Human BD Fc Block (BD). Cells were stained
182 using the antibodies listed in **Supplementary Table 1** for 15 minutes in the dark at room
183 temperature and washed three times with FCM buffer. Finally, cells were resuspended in
184 200 μL of FCM buffer including 20 μL 7-amino-actinomycin D (7-AAD) viability
185 staining solution (BD) and incubated for 10-30 minutes before acquisition. A BD
186 FACSCalibur cell analyzer and BD CellQuest version 6.0 software (BD) were used for
187 FCM analysis. Gates for cells staining with antibody were set so that isotype control
188 staining was less than 5% of events.
189
190 **Enzyme-Linked Immunosorbent Assay (ELISA)**
191 To evaluate the cytokine levels in cell culture supernatants, ELISA for human IL-6 and

192 IL-10 were performed using ELISA kits (DuoSet [R&D Systems] or BD OptEIA [BD])
193 following the manufacturer's instructions. Absorbance at 450 nm (subtracted absorbance
194 at 540 nm) was detected using a Spark 10M (TECAN). The assay ranges for the kits are:
195 IL-6 (9.38-600 pg/mL [DuoSet], 4.7-300 pg/mL [OptEIA]) and IL-10 (31.3-2000 pg/mL
196 [DuoSet], 7.8-500 pg/mL [OptEIA]).
197
198 **Western blotting**
199 Cells (2 x 10^6 cells) were harvested by centrifugation, washed with PBS, and lysed in
200 RIPA buffer (50 mM Tris-HCl pH 8.0, 150 mM NaCl, 2 mM EDTA, 1% Nonidet P-40
201 [NP-40], 0.5% sodium deoxycholate, 0.1% SDS, cOmplete, EDTA-free protease inhibitor
202 cocktail (Roche), and phosphatase inhibitor cocktail solution I (Wako)). After removal of
203 nuclear pellets by centrifugation, cell lysate supernatants were mixed with sample buffer
204 (final 62.5 mM Tris-HCl pH 6.8, 25% (v/v) glycerol, 2.5% (w/v) SDS, 0.0125% (w/v)
205 bromophenol blue, and 5% 2-mercaptoethanol (2-ME)), separated on the 12.5% or 10%
206 acrylamide gel, and transferred to PVDF membrane (Bio-Rad). Antibodies used in this
207 study are shown in **Supplementary Table 1**. ECL prime western blotting detection
208 reagent (GE Healthcare) and ImageQuant LAS4000mini (GE Healthcare) were used for
209 detection. IDO-1, STAT3, phosphorylated STAT3 and β-actin (as a loading control) were
210 detected on the same membrane by reprobing with antibodies after stripping with
211 stripping buffer (62.5 mM Tris-HCl pH 6.8, 2% SDS, and 0.7% 2-ME).

212

213 **Surface plasmon resonance (SPR)**

214 SPR analysis was performed using a BIAcore2000 (GE Healthcare) at 25°C. C-
215 terminally biotinylated LILRB2 and BSA (negative control, Wako) were prepared as
216 previously described (24). Biotinylated proteins were immobilized on a CAP chip (Biotin
217 CAPture kit, GE Healthcare). As a blocking control anti-LILRB2 antibody, clone 27D6
218 (IgM, Thermo Fisher Scientific) was repeatedly injected until binding to immobilized
219 LILRB2 reached saturation. Then, purified HLA-G2 (3.6 μM) in HBS-EP was injected
220 over either LILRB2, LILRB2 blocked with 27D6 antibody, or BSA (negative control) for
221 3 min. The flow rate was 10 μL/min.

222

223 **Blocking assay**

224 CD14-positive monocytes isolated from human PBMCs (1 x 10^6 cells/well) were
225 incubated with 27D6 antibody or isotype-matched control antibody (4 μg/mL, IgM,
226 Thermo Fisher Scientific) for 30 min at room temperature, then cultured in 10% FBS
227 RPMI-1640 with 2.3 μM HLA-G2 or PBS for two days. IDO-1 and β-actin (loading
228 control) in the cell lysates were detected by western blotting, and IL-6 and IL-10 in the
229 cell culture supernatants were evaluated by ELISA as described above.

230

231 **Allogeneic Mixed Lymphocyte Reaction (MLR)**

232 IFN-DCs incubated with 2.3 μM HLA-G2 or PBS for 48 hours were treated with 10
233 μg/mL of mitomycin C (Nacalai tesque). CD14-negative PBMC lymphocytes isolated
234 from a different healthy donor were labelled with CFSE to monitor proliferation. CFSE-
235 labelled lymphocytes were co-cultured with IFN-DCs for two days with 100 U/mL IL-2
236 at a ratio of 10:1 ($2x10^6$ cells lymphocytes: $2x10^5$ cells IFN-DC). After 48 hours,
237 proliferating CD3-positive cells were evaluated by FCM using carboxyfluorescein
238 diacetate succinimidyl ester (CFSE) as a proliferation marker.
239
240 **Autologous MLR**
241 IFN-DCs generated from a HLA-A*0201-positive donor were stimulated with 2.3 μM
242 HLA-G2 or PBS for two days, and cultured overnight with a Melan-A/MART-1_{26-35}
243 antigenic peptide analogue incorporating an Ala27 to Leu mutation (MART-1(A27L),
244 ELAGIGILTV) (25-27). Subsequently, IFN-DCs were harvested and incubated with
245 lymphocytes from the same donor in RPMI-1640 medium with 10% FBS and IL-2 (100
246 U/mL) at a 10:1 ratio (2×10^6 cells lymphocytes: 2×10^5 IFN-DCs). After 14 days, CD8-
247 positive MART-1(A27L) peptide-specific T cells were evaluated by FCM by staining
248 with PE-conjugated MART-1(A27L) tetramer and anti-CD8 FITC (BioLegend)
249 (**Supplementary Table 1**).
250

251 **Results**

252 **HLA-G2 induced an immunosuppressive phenotype in human monocytes.**

253 Recombinant HLA-G2 homodimer protein was prepared as previously described
254 (**Supplementary Figure 2**) (8, 12). LILRB2, a functional receptor for HLA-G2, was
255 constitutively expressed on CD14-positive monocytes isolated from PBMCs (82 ± 16%,
256 $n = 8$) (**Figure 1A**). CD14-positive monocytes were cultured with the recombinant HLA-
257 G2 protein (2.3 μM final concentration in PBS) or with PBS as described in Materials
258 and Methods. The expression of HLA-DR and the co-stimulatory molecule CD86 was
259 significantly down-regulated by incubation with HLA-G2 for 48 hours (**Figure 1B, C**).
260 Notably, the immune checkpoint molecule, PD-L1, was up-regulated by HLA-G2
261 treatment (**Figure 1B, C**). Although upregulation of PD-L1 was clearly observed after
262 treatment with HLA-G2 for 18 hours, changes in cell surface expression of HLA-DR and
263 CD86 did not appear until a later time point (**Supplementary Figure 3A**).

264 In order to evaluate the molecular mechanism of HLA-G2 signaling, levels of the
265 immunosuppressive cytokine, IL-10, and stimulation of IL-6/STAT3/IDO pathway were
266 determined. Upregulation of IL-6 by monocytes was observed from 8 hours and increased
267 with time and dose following HLA-G2 treatment (**Figure 1D, Supplementary Figure**
268 **3B-D**). Furthermore, the immunosuppressive cytokine, IL-10, was also upregulated by
269 HLA-G2 (**Figure 1D, Supplementary Figure 3D**). Phosphorylation of STAT3 and
270 expression of IDO-1 were also upregulated by HLA-G2 treatment (**Figure 1E**). Thus,

271 HLA-G2 treatment affects similar signaling pathways to HLA-G1-LILRB2 (19, 21, 22),
272 and elicits immunological tolerance in human peripheral blood monocytes.
273
274 **HLA-G2 binding to LILRB2 is blocked with anti-LILRB2 antibody.**
275 To determine whether the immunosuppressive phenotype induced by HLA-G2 could be
276 mediated by binding to the HLA-G2 receptor, LILRB2, HLA-G2 binding to LILRB2 was
277 first assayed in the presence of anti-LILRB2 antibody. Previously the anti-
278 LILRB2 monoclonal antibody, 27D6 (Thermo Fisher Scientific), has been shown to block
279 HLA-G1−LILRB2 binding (28). Thus, the ability of the 27D6 antibody to block HLA-
280 G2−LILRB2 binding was analyzed by surface plasmon resonance (SPR) analysis (**Figure**
281 **2A**). The HLA-G2 binding response to LILRB2 bound to 27D6 antibody (black line) was
282 dramatically reduced compared to the response to LILRB2 (gray line) (**Figure 2A**),
283 indicating that 27D6 antibody blocks HLA-G2 binding to LILRB2. We then examined
284 the expression profiles of signaling molecules in human monocyte and treated with HLA-
285 G2. The 27D6 antibody blocked IL-6 and IL-10 upregulation, and IDO-1 expression
286 induced in HLA-G2 treated monocytes (**Figure 2B, C**). Thus, induction of the
287 immunosuppressive monocyte phenotype by HLA-G2 was mediated by HLA-G2 binding
288 to LILRB2.
289
290 **Induction of Tolerogenic IFN-DCs by HLA-G2−LILRB2 signaling.**

291 In order to determine whether HLA-G2 could also affect DC function, the levels of
292 LILRB2 expression on PBMC-derived DCs were first determined. As previously reported
293 (19), compared with monocytes (**Figure 1A)**, LILRB2 expression on IL-4-DCs was
294 dramatically decreased following differentiation, while IFN-DCs maintained expression
295 of LILRB2 (**Figure 3A**). Thus, the effect of HLA-G2 on DC phenotype was investigated
296 using IFN-DCs. As observed with monocytes (**Figure 1**), HLA-G2 treatment also induced
297 significant up-regulation of PD-L1 expression in IFN-DCs, but by contrast, HLA-DR and
298 CD86 expression did not show any substantial change in expression (**Figure 3B**).
299 Furthermore, HLA-G2 treatment enhanced production of IL-6 and IL-10 (**Figure 3C**).
300 To examine the effect of HLA-G2 treatment on the function of IFN-DCs, mixed
301 lymphocyte reaction (MLR) analyses were performed. IFN-DCs were first incubated with
302 HLA-G2 or PBS for 48 hours, then cocultured with CFSE-labelled CD14-negative
303 lymphocytes containing T cells from a different donor for further six days. The percentage
304 of proliferating CD3-positive T cells incubated with HLA-G2-treated IFN-DCs (9.2%)
305 was lower than that incubated with PBS-treated IFN-DCs (19.0%) (**Figure 4A**). Next,
306 autologous MLR assays using a melanoma antigen peptide, MART-1(A27L), specific to
307 HLA-A*0201 was performed. The MART-1(A27L) peptide-loaded HLA-G2-treated
308 IFN-DC and CFSE-labelled lymphocytes from the same HLA-A:0201-positive donors
309 were cocultured, and the population of the proliferating MART-1(A27L)-specific $CD8^{high}$
310 T cells was compared. The $CD8^{high}$ cells staining with MART-1(A27L) tetramer was

311 decreased by co-culture with IFN-DCs (1.2%) treated with HLA-G2, compared to PBS-

312 treated IFN-DCs (8.2%) (**Figure 4B**). These results show that HLA-G2-treated IFN-DCs

313 are functionally tolerogenic and inhibit the proliferation of T lymphocytes.

314 **DISCUSSION**

315 Here we demonstrated the immunosuppressive effects of HLA-G2 binding to LILRB2
316 expressed on human peripheral blood monocytes and monocyte-derived IFN-DCs. To
317 understand the molecular mechanism of immunosuppressive function induced by HLA-
318 G2 treatment, we evaluated the expression profiles of representative cell surface
319 molecules on human antigen presenting cells. HLA-G2 treatment down-regulated the
320 expression of cell surface activation markers, CD86 and HLA-DR, on monocytes
321 (**Figures 1B, C**). Notably, we observed substantial upregulation of PD-L1 on both
322 monocytes and IFN-DCs (**Figures 1B, C, Figure 3B, Supplementary Figure 3A**). Since
323 blocking the important PD-1/PD-L1 immune checkpoint pathway has shown promising
324 results in clinical trials for various cancers (29), the observations in this study strongly
325 suggest that the HLA-G2 binding to LILRB2 can be an important immune checkpoint
326 pathway.

327 In regard to intracellular signaling, we showed that HLA-G2−LILRB2 interaction
328 induced IL-6−STAT3−IDO-1 signaling in human antigen presenting cells (APCs)
329 (**Figure 1**). While IL-6 has long been known as a potent proinflammatory cytokine in T
330 cell activation (30), IL-6 can also have immunosuppressive functions, especially in the
331 tumor microenvironment (31). Indeed, IL-6-STAT3 signaling inhibits DC maturation (32,
332 33) and IL-6−STAT3−IDO-1 signaling is activated in myeloid-derived suppressor cells
333 (34). Furthermore, during DC differentiation, STAT3 is involved in the upregulation of

334 PD-L1 in the differentiation of tolerogenic APCs (35). HLA-G2 binding to LILRB2 could
335 be one mechanism by which IL-6 induces suppressive immune cells, as we showed with
336 human monocytes and IFN-DCs in this study (**Figure 1D, Figure3C, Supplementary**
337 **Figure 3B-D**).

338 The induction of human myelomonocytic cells with an immunosuppressive phenotype
339 by HLA-G2 treatment could be blocked with anti-LILRB2 antibody (**Figure 2**). The
340 molecular mechanism of the immunosuppressive effect of LILRB2 ligation by HLA-G
341 has only been reported using the most conventional HLA-G isoform, HLA-G1. In
342 LILRB2 transgenic mice, HLA-G1 downregulated HLA-DR in DCs through the
343 upregulation of IL-6 and IL-10 as well as STAT3 activation (21). Thus, we propose a
344 potential molecular signaling network where HLA-G2 binding to LILRB2 leads to the
345 induction of PD-L1 expression (**Figure 5**). The phosphorylated ITIMs of LILRB2
346 possibly recruit SHP-2 phosphatase (21). Subsequently, IL-6 and IL-10 would be up-
347 regulated by NF-κB-related signaling to act in an autocrine manner as proposed in HLA-
348 G1−LILRB2 signaling pathway model (21). Following this, STAT3 activation would lead
349 to up-regulation of PD-L1, induction of IDO-1, and consecutive downregulation of HLA
350 class II and CD86 (**Figure 5**). To further understand the molecular mechanisms of HLA-
351 G2-induced immune suppression, a more detai functional relationship between immune
352 checkpoint molecules, such as PD-L1-related molecules, needs to be elucidated.

353 Although the LILRB2 signaling by HLA-G1 and -G2 are similar as mentioned above,

354 their receptor preference is clearly different. HLA-G1 can bind to both LILRB1 and
355 LILRB2, however, HLA-G2 only binds to LILRB2. Thus, HLA-G2 functional effects are
356 restricted to LILRB2-positive myeloid APCs but HLA-G1 can more broadly affect the
357 function of LILRB1- and LILRB2-positive immune cells (APCs, B cells, NK cells and T
358 cells). In mice, both HLA-G1 and HLA-G2 recombinant proteins bound to PIR-B, which
359 is a mouse orthologue of LILRB2, and expressed on myeloid APCs and B cells. The
360 immunosuppressive effects of HLA-Gs in mice immune inflammation models suggests
361 that the direct suppression of T and NK cells is not essential to reduce autoimmune
362 pathology (12, 16). When HLA-G2 is administered to humans, it binds only to LILRB2
363 expressed on APCs, so it likely induces more specific immune suppression than HLA-G1.
364 Interestingly, the immunosuppressive effect in CIA mice was observed by the
365 administration of less recombinant HLA-G2 protein than HLA-G1 and could possibly be
366 due to higher affinity of HLA-G2 for PIR-B (11, 12). Regarding human LILRB2 binding,
367 HLA-G2 showed higher affinity than HLA-G1 due to an avidity effect (8). Thus, in terms
368 of the development of biopharmaceuticals for autoimmune disorders, HLA-G2 might be
369 more suitable for clinical use in respect of the more restricted target specificity and higher
370 receptor binding affinity.

371 HLA-G has recently been considered as a target for novel combined immunotherapies.
372 Some tumors have been reported to express various soluble HLA-G molecules, such as
373 β2m-free form of HLA-G1, the disulfide-bonded homodimer isoforms of HLA-G1, and

374 HLA-G2 to suppress immune cell surveillance functions as summarized by Dias, F.C. et
375 al (36). In epithelial cell adhesion molecule-positive colorectal cancer cells, not only PD-
376 L1 but both LILRB2 and HLA-G were upregulated and associated with lymph node
377 metastasis (37). Consistently, we showed that HLA-G2-treated IFN-DCs inhibited T cell
378 proliferation against both auto- and allo-antigens in MLR assays (**Figure 4**). Thus, our
379 results raise the possibility that blocking HLA-G2−LILRB2 signaling could be an
380 effective cancer treatment especially for the non- and low-responders to PD-1/PD-L1
381 therapy. Interestingly, the importance of PD-L1 expression in the accumulation of
382 senescent cells and inflammation associated with aging was reported as a new aspect of
383 PD-L1 signaling (38). The molecular relationship between HLA-G2−LILRB2−PD-L1
384 signaling and the regulation of expression of these molecules and inflammation in aging
385 is worthy of future study.

386 The present study showed the LILRB2 signaling by binding to HLA-G2 induced broad
387 immune suppression and a tolerogenic phenotype in human CD14-positive monocytes
388 and monocyte-derived IFN-DCs. These results suggest the functional importance of the
389 HLA-G2 isoform and LILRB2 as immune checkpoint molecules. Thus, the HLA-
390 G2−LILRB2 signaling pathway might be a promising target to regulate pathological
391 immune responses in immune checkpoint-related diseases, such as autoimmune diseases
392 and cancers. In summary, HLA-G2 modulates human immune responses by the induction
393 of immunosuppressive monocytes and DCs with increased PD-L1 expression.

Acknowledgement

We thank Y. Eiraku, T. Tadokoro for technical support and S. Kollnberger for helpful discussions.

Grant Support

This study was partly supported by the MEXT/JSPS KAKENHI Grant Number JP20H05873, and by the Japan Agency for Medical Research and Development (AMED) under Grant Numbers JP22ama121037, JP223fa627005, JP22gm1810004, Hokkaido University, Global Facility Center, Pharma Science Open Unit, funded by Ministry of Education, Culture, Sports, Science and Technology Grant "Support Program for Implementation of New Equipment Sharing System," Hokkaido University Biosurface Project, Takeda Science Foundation, and Japan Society for the Promotion of Science KAKENHI Grants 25870019, 18K06073, 22H02749 and 16J05871. K.K. is supported by The Naito Foundation.

Author contributions

A.T., K.K., M.N., and K.M. designed the experiments, performed research, and analyzed the data. A.T., K.K., and K.M. wrote the paper.

413 **Figure Legends**

414 **Figure 1 HLA-G2 induces human CD14-positive monocytes with an**
415 **immunosuppressive phenotype.**

416 A. Flow cytometry analysis of surface LILRB2 expression by purified $CD14^+$ monocytes
417 (open histogram). Gray-filled histogram represents isotype control. Representative
418 data of eight experiments from seven donors are shown.

419 B. Flow cytometry histogram analyses of HLA-DR, CD86 and PD-L1 expression (open
420 histogram) of $CD14^+$ monocytes either untreated or following treatment with PBS on
421 HLA-G2 as indicated. Gray-filled histograms represent isotype control.
422 Representative data of seven donors are shown. ΔMFI (MFI of target molecule – MFI
423 of isotype-matched control) are shown in the upper right side.

424 C. Box and superimposed dot plot showing the MFI ratio from (B) of $CD14^+$ monocytes
425 either untreated or in response to treatment with PBS or HLA-G2 as indicated. MFI
426 ratio was calculated by (ΔMFI of PBS or HLA-G2)/ ΔMFI of non-treated control (n=
427 8). The boxes indicate the first and third quartiles. The bold line in the boxes indicates
428 median values.

429 D. IL-6 (upper) and IL-10 (lower) production in monocytes with/without HLA-G2
430 treatment. Representative data (average with standard deviation from two
431 independent experiments) of three individuals are shown.

432 E. STAT3 activation and IDO expression in response to HLA-G2 treatment.

433 Representative data from three independent experiments are shown.

434

435 **Figure 2 HLA-G2 binding to LILRB2 and induction of monocytes with an**

436 **immunosuppressive phenotype are inhibited by LILRB2 antibody blockade.**

437 A. Left panel. SPR analysis of biotinylated BSA (control, gray dot line) or LILRB2

438 (black and gray solid lines) immobilized on a CAP chip via streptavidin (700 RU),

439 and saturated with anti-LILRB2 (27D6) by repeated injection to cover the

440 immobilized LILRB2 (black solid line). Right panel. SPR analyses showing binding

441 responses of HLA-G2 against BSA (negative control), LILRB2 (positive control) and

442 LILRB2 saturated with 27D6 antibody after Y-axis transformation at zero RU before

443 injection.

444 B. IL6 (upper) and IL-10 (lower) production by $CD14^+$ monocytes in response to HLA-

445 G2 treatment (2.3 μM) with or without 27D6 antibody. Representative data from three

446 independent experiments using monocytes isolated from one individual.

447 C. IDO expression by $CD14^+$ monocytes in response to HLA-G2 treatment (2.3 μM)

448 with or without 27D6 antibody. Representative data from three independent

449 experiments.

450

451 **Figure 3 HLA_G2 induces IFN-Dendritic Cells (IFN-DC) with an**

452 **immunosuppressive phenotype.**

453 A. Flow cytometry analysis of cell surface LILRB2 expression by IL-4 and IFN
454 differentiated DC (black-filled histogram). Open histograms show staining with
455 isotype control. Representative data from two individuals.
456 B. Flow cytometry histogram analyses of HLA-DR, CD86 and PD-L1 expression (black-
457 filled histogram) by IFN-DC either untreated or treated with PBS or HLA-G2 as
458 indicated. Open histograms show staining with isotype control. Representative data
459 of three independent experiments from one individual.
460 C. IL-6 (left) and IL-10 (right) production by IFN-DCs with/without HLA-G2 (2.3 μM)
461 treatment. Mean values with standard deviation from three independent experiments
462 from one individual.
463
464 **Figure 4 MLR of HLA-G2-treated IFN-DCs**
465 A. Allogenic MLR analysis of CFSE-labelled T lymphocyte proliferation in response to
466 IFN-DCs treated with or without HLA-G2 (2.3 μM) treatment. Dot plots show healthy
467 donor $CD3^+$ T cell proliferation after six days culture with treated or untreated IFN-
468 DC and IL-2 from a different healthy donor. The percentage of $CD4^+CD3^+$ T cells are
469 shown in the left upper panels. Representative data from two independent
470 experiments using two different healthy donor pairs are shown.
471 B. Autologous MLR analysis of CD8 T lymphocyte proliferation in response to culture
472 with IL-2 and peptide-pulsed IFN-DCs from the same donor with or without HLA-

473 G2 (2.3 μM) treatment. Dot blots show proliferation of CD8-positive T cells after 14-
474 day stimulation. The percentage of CD8 positive T cells staining with MART-1
475 (A27L) tetramers cells are shown in the upper right quadrants. Plots show
476 representative data from two independent experiments from one healthy HLA-A2-
477 positive individual.
478
479 **Figure 5. Model of the immunosuppressive mechanism of HLA-G2 in LILRB2-**
480 **positive myelomonocytic cells**
481
482 **Supplementary Figure 1. Schematic structures of HLA-G isoform proteins.**
483 The alternative splicing of the primary HLA-G transcript generates seven isoforms. HLA-
484 G1 to HLA-G4 isoforms have a transmembrane region (membrane-bound forms),
485 whereas HLA-G5 to HLA-G7 isoforms have an intron-encoded region at the C-terminus
486 shown as a grey stalk region.
487
488 **Supplementary Figure 2. Preparation of HLA-G2 homodimer.**
489 A. HLA-G2 homodimer was purified by gel filtration chromatography on a HiLoad26/60
490 Superdex 75 column (42 kDa in dimer, left).
491 B. The peak indicated by a black arrow in A. was analyzed by SDS-PAGE under non-
492 reducing condition (21 kDa in monomer). A faint band around 42 kDa indicates

493 further oligomerization, such as a disulfide-linked dimer of HLA-G2 homodimer.

494

495 **Supplementary Figure 3. Time and dose-dependence of HLA-G2 induction of**

496 **human CD14$^+$ monocytes with an immunosuppressive phenotype.**

497 A. Flow cytometry histogram analyses of HLA-DR, CD86 and PD-L1 expression (open

498 histogram) by CD14$^+$ positive monocytes in response to HLA-G2 treatment for 18

499 hours. Gray-filled histograms show isotype control antibody staining. Representative

500 data from three independent experiments are shown. ΔMFI (MFI of target molecule

501 – MFI of isotype-matched control) are shown in the upper right of the plots.

502 B. IL-6 production by HLA-G2 treatment (0.58, 1.2 and 2.3 μM) of CD14$^+$ monocytes

503 for 48 hours.

504 C. IL-6 production by HLA-G2 treatment (2.3 μM) of CD14$^+$ monocytes for one hour

505 and 8 hours.

506 D. IL-10 (left) and IL-6 (right) production by HLA-G2 treatment (2.3 μM) of CD14$^+$

507 monocytes for 18 and 48 hours.

508 B-D. Data are representative data from duplicate experiments with CD14$^+$ monocytes

509 from one individual.

510

511 **References**

512 1. Donadi EA*, et al.* (2011) Implications of the polymorphism of HLA-G on its
513 function, regulation, evolution and disease association. *Cell Mol Life Sci* 68(3):369-395.

514 2. Kamishikiryo J & Maenaka K (2009) HLA-G molecule. *Curr Pharm Des*
515 15(28):3318-3324.

516 3. Kuroki K & Maenaka K (2007) Immune modulation of HLA-G dimer in
517 maternal-fetal interface. *Eur J Immunol* 37(7):1727-1729.

518 4. Hunt JS, Petroff MG, McIntire RH, & Ober C (2005) HLA-G and immune
519 tolerance in pregnancy. *FASEB J* 19(7):681-693.

520 5. Crisa L, McMaster MT, Ishii JK, Fisher SJ, & Salomon DR (1997)
521 Identification of a thymic epithelial cell subset sharing expression of the class Ib HLA-G
522 molecule with fetal trophoblasts. *J Exp Med* 186(2):289-298.

523 6. Feger U*, et al.* (2007) HLA-G expression defines a novel regulatory T-cell
524 subset present in human peripheral blood and sites of inflammation. *Blood* 110(2):568-
525 577.

526 7. Gonzalez A*, et al.* (2012) The immunosuppressive molecule HLA-G and its
527 clinical implications. *Crit Rev Clin Lab Sci* 49(3):63-84.

528 8. Kuroki K*, et al.* (2017) Cutting Edge: Class II-like Structural Features and
529 Strong Receptor Binding of the Nonclassical HLA-G2 Isoform Homodimer. *J Immunol*
530 198(9):3399-3403.

531 9. Shiroishi M, *et al.* (2003) Human inhibitory receptors Ig-like transcript 2 (ILT2)
532 and ILT4 compete with CD8 for MHC class I binding and bind preferentially to HLA-G.
533 *Proc Natl Acad Sci U S A* 100(15):8856-8861.
534 10. Hudson LE & Allen RL (2016) Leukocyte Ig-Like Receptors - A Model for
535 MHC Class I Disease Associations. *Front Immunol* 7:281.
536 11. Kuroki K, *et al.* (2013) The long-term immunosuppressive effects of disulfide-
537 linked HLA-G dimer in mice with collagen-induced arthritis. *Hum Immunol* 74(4):433-
538 438.
539 12. Takahashi A, *et al.* (2016) The immunosuppressive effect of domain-deleted
540 dimer of HLA-G2 isoform in collagen-induced arthritis mice. *Hum Immunol* 77(9):754-
541 759.
542 13. Matsushita H, *et al.* (2011) Differential but competitive binding of Nogo protein
543 and class i major histocompatibility complex (MHCI) to the PIR-B ectodomain provides
544 an inhibition of cells. *J Biol Chem* 286(29):25739-25747.
545 14. Liang S, Baibakov B, & Horuzsko A (2002) HLA-G inhibits the functions of
546 murine dendritic cells via the PIR-B immune inhibitory receptor. *Eur J Immunol*
547 32(9):2418-2426.
548 15. Maeda N, Yamada C, Takahashi A, Kuroki K, & Maenaka K (2017)
549 Therapeutic application of human leukocyte antigen-G1 improves atopic dermatitis-like
550 skin lesions in mice. *Int Immunopharmacol* 50:202-207.

551 16. Watanabe H, *et al.* (2019) Therapeutic effects of soluble human leukocyte
552 antigen G2 isoform in lupus-prone MRL/lpr mice. *Hum Immunol*.
553 17. Bahri R, *et al.* (2006) Soluble HLA-G inhibits cell cycle progression in human
554 alloreactive T lymphocytes. *J Immunol* 176(3):1331-1339.
555 18. Naji A, *et al.* (2014) Binding of HLA-G to ITIM-bearing Ig-like transcript 2
556 receptor suppresses B cell responses. *J Immunol* 192(4):1536-1546.
557 19. Ristich V, Liang S, Zhang W, Wu J, & Horuzsko A (2005) Tolerization of
558 dendritic cells by HLA-G. *Eur J Immunol* 35(4):1133-1142.
559 20. Ristich V, Zhang W, Liang S, & Horuzsko A (2007) Mechanisms of
560 prolongation of allograft survival by HLA-G/ILT4-modified dendritic cells. *Hum*
561 *Immunol* 68(4):264-271.
562 21. Liang S, *et al.* (2008) Modulation of dendritic cell differentiation by HLA-G
563 and ILT4 requires the IL-6--STAT3 signaling pathway. *Proc Natl Acad Sci U S A*
564 105(24):8357-8362.
565 22. Lee CL, *et al.* (2015) Soluble human leukocyte antigen G5 polarizes
566 differentiation of macrophages toward a decidual macrophage-like phenotype. *Hum*
567 *Reprod* 30(10):2263-2274.
568 23. Nieda M, Terunuma H, Eiraku Y, Deng X, & Nicol AJ (2015) Effective
569 induction of melanoma-antigen-specific CD8+ T cells via Vgamma9gammadeltaT cell
570 expansion by CD56(high+) Interferon-alpha-induced dendritic cells. *Exp Dermatol*

571 24(1):35-41.

572 24. Shiroishi M, *et al.* (2006) Efficient leukocyte Ig-like receptor signaling and
573 crystal structure of disulfide-linked HLA-G dimer. *J Biol Chem* 281(15):10439-10447.

574 25. Men Y, *et al.* (1999) Assessment of immunogenicity of human Melan-A peptide
575 analogues in HLA-A*0201/Kb transgenic mice. *J Immunol* 162(6):3566-3573.

576 26. Valmori D, *et al.* (1998) Enhanced generation of specific tumor-reactive CTL
577 in vitro by selected Melan-A/MART-1 immunodominant peptide analogues. *J Immunol*
578 160(4):1750-1758.

579 27. Valmori D, *et al.* (2000) Induction of potent antitumor CTL responses by
580 recombinant vaccinia encoding a melan-A peptide analogue. *J Immunol* 164(2):1125-
581 1131.

582 28. Allan DS, *et al.* (1999) Tetrameric complexes of human histocompatibility
583 leukocyte antigen (HLA)-G bind to peripheral blood myelomonocytic cells. *J Exp Med*
584 189(7):1149-1156.

585 29. Zhang M, *et al.* (2017) PD-L1 expression in lung cancer and its correlation with
586 driver mutations: a meta-analysis. *Sci Rep* 7(1):10255.

587 30. Kang S, Tanaka T, Narazaki M, & Kishimoto T (2019) Targeting Interleukin-6
588 Signaling in Clinic. *Immunity* 50(4):1007-1023.

589 31. Fisher DT, Appenheimer MM, & Evans SS (2014) The two faces of IL-6 in the
590 tumor microenvironment. *Semin Immunol* 26(1):38-47.

591 32. Hunter CA & Jones SA (2015) IL-6 as a keystone cytokine in health and disease.
592 *Nat Immunol* 16(5):448-457.
593 33. Scheller J, Chalaris A, Schmidt-Arras D, & Rose-John S (2011) The pro- and
594 anti-inflammatory properties of the cytokine interleukin-6. *Biochim Biophys Acta*
595 1813(5):878-888.
596 34. Yu J*, et al.* (2014) Noncanonical NF-kappaB activation mediates STAT3-
597 stimulated IDO upregulation in myeloid-derived suppressor cells in breast cancer. *J*
598 *Immunol* 193(5):2574-2586.
599 35. Wolfle SJ*, et al.* (2011) PD-L1 expression on tolerogenic APCs is controlled by
600 STAT-3. *Eur J Immunol* 41(2):413-424.
601 36. Dias FC, Castelli EC, Collares CV, Moreau P, & Donadi EA (2015) The Role
602 of HLA-G Molecule and HLA-G Gene Polymorphisms in Tumors, Viral Hepatitis, and
603 Parasitic Diseases. *Front Immunol* 6:9.
604 37. Chen QY*, et al.* (2021) Prognostic Significance of Immune Checkpoints HLA-
605 G/ILT-2/4 and PD-L1 in Colorectal Cancer. *Front Immunol* 12:679090.
606 38. Wang TW, et al. (2022) Blocking PD-L1-PD-1 improves senescence
607 surveillance and ageing phenotypes. Nature 611(7935):358-364.
608

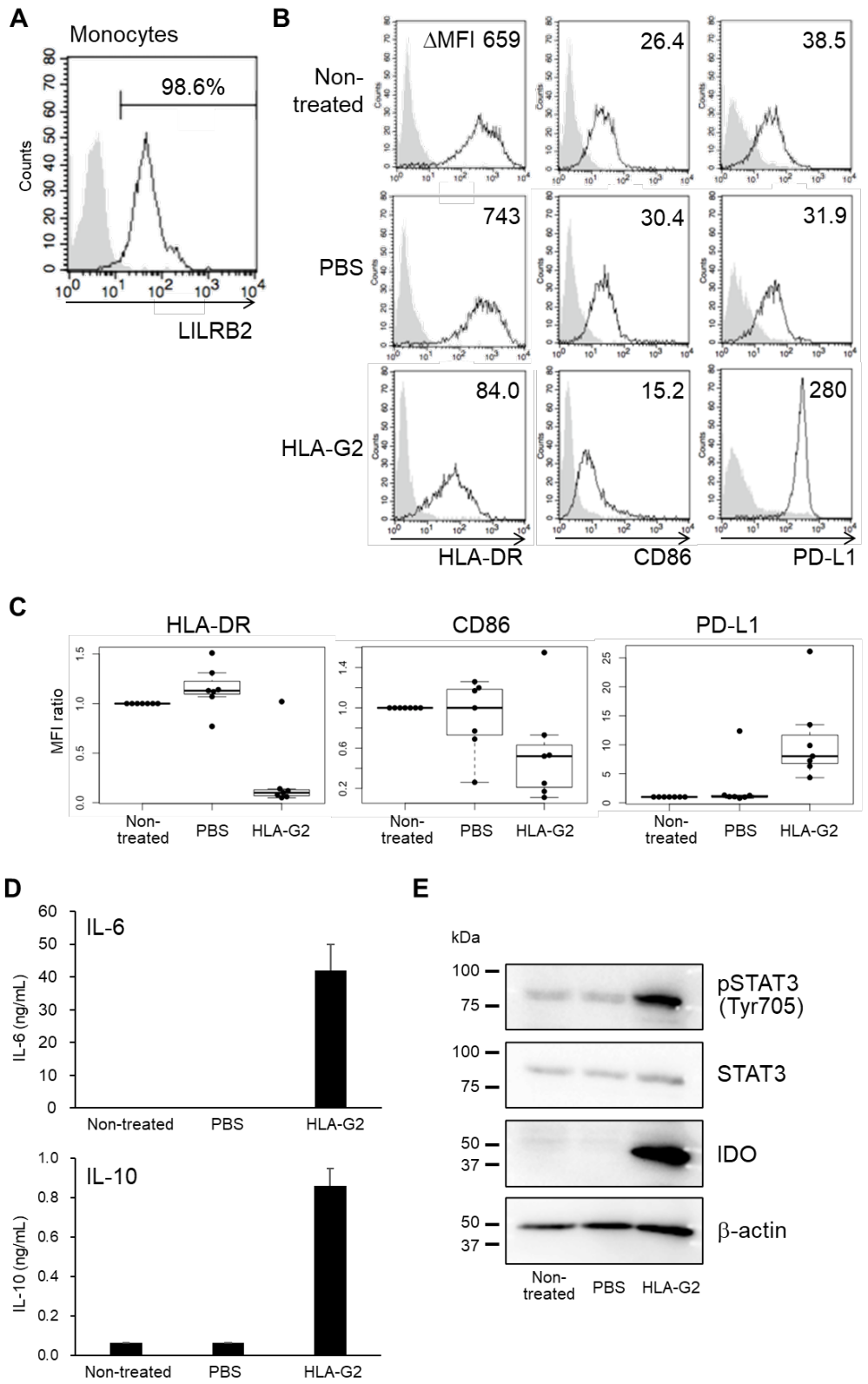

Figure 1. HLA-G2 induces human CD14-positive monocytes with an immunosuppressive phenotype.
A. Flow cytometry analysis of surface LILRB2 expression by purified CD14$^+$ monocytes (open histogram). Gray-filled histogram represents isotype control. Representative data of eight experiments from seven donors are shown.
B. Flow cytometry histogram analyses of HLA-DR, CD86 and PD-L1 expression (open histogram) of CD14$^+$ monocytes either untreated or following treatment with PBS on HLA-G2 as indicated. Gray-filled histograms represent isotype control. Representative data of seven donors are shown. ΔMFI (MFI of target molecule – MFI of isotype-matched control) are shown in the upper right side.
C. Box and superimposed dot plot showing the MFI ratio from (B) of CD14$^+$ monocytes either untreated or in response to treatment with PBS or HLA-G2 as indicated. MFI ratio was calculated by (ΔMFI of PBS or HLA-G2)/ ΔMFI of non-treated control (n= 8). The boxes indicate the first and third quartiles. The bold line in the boxes indicates median values.
D. IL-6 (upper) and IL-10 (lower) production in monocytes with/without HLA-G2 treatment. Representative data (average with standard deviation from two independent experiments) of three individuals are shown.
E. STAT3 activation and IDO expression in response to HLA-G2 treatment. Representative data from three independent experiments are shown.

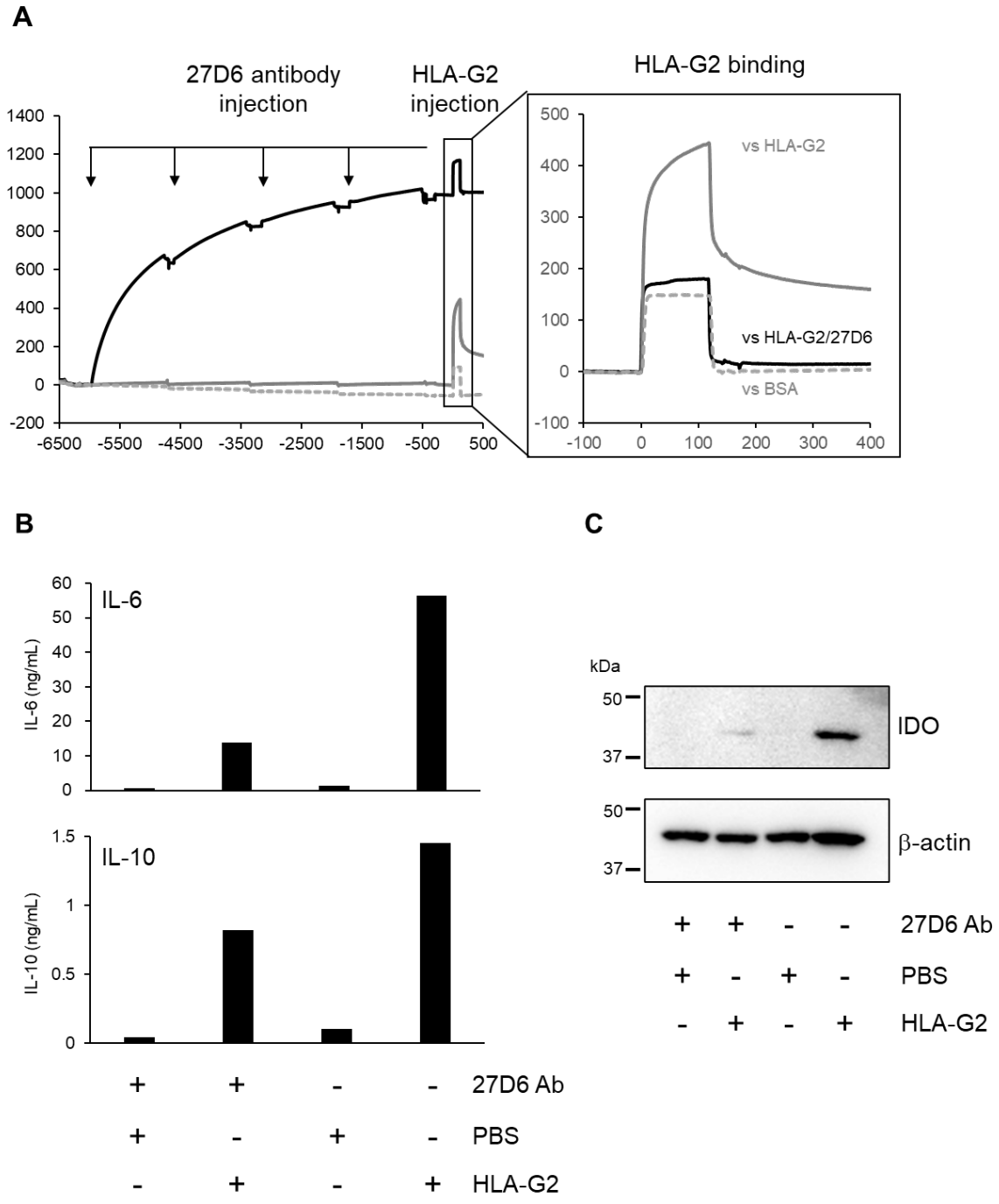

Figure 2. HLA-G2 binding to LILRB2 and induction of monocytes with an immunosuppressive phenotype are inhibited by LILRB2 antibody blockade.

A. Left panel. SPR analysis of biotinylated BSA (control, gray dot line) or LILRB2 (black and gray solid lines) immobilized on a CAP chip via streptavidin (700 RU), and saturated with anti-LILRB2 (27D6) by repeated injection to cover the immobilized LILRB2 (black solid line). Right panel. SPR analyses showing binding responses of HLA-G2 against BSA (negative control), LILRB2 (positive control) and LILRB2 saturated with 27D6 antibody after Y-axis transformation at zero RU before injection.

B. IL6 (upper) and IL-10 (lower) production by CD14+ monocytes in response to HLA-G2 treatment (2.3 μM) with or without 27D6 antibody. Representative data from three independent experiments using monocytes isolated from one individual are shown.

C. IDO expression by CD14+ monocytes in response to HLA-G2 treatment (2.3 μM) with or without 27D6 antibody. Representative data from three independent experiments is shown.

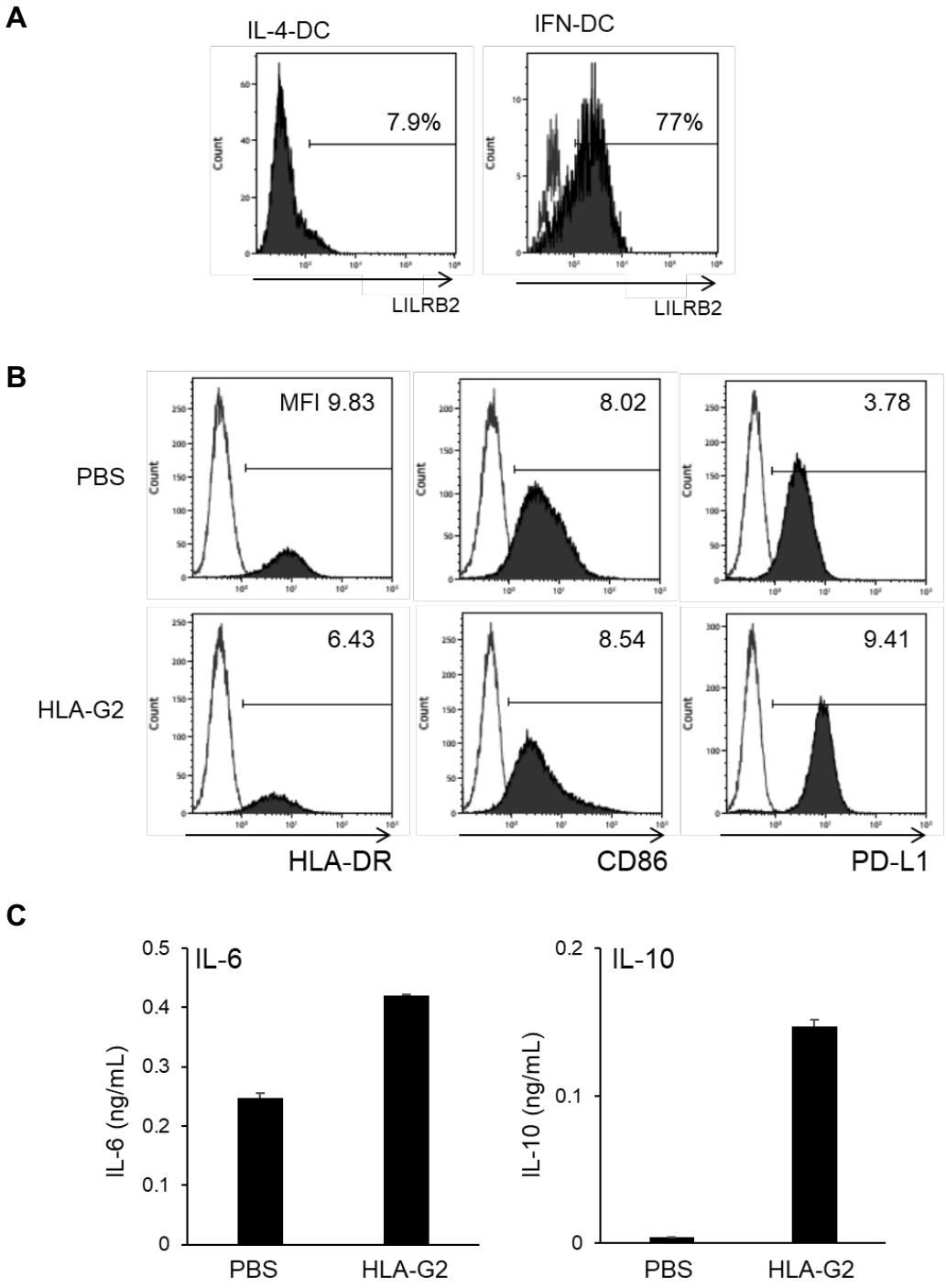

Figure 3. HLA_G2 induces IFN-Dendritic Cells (IFN-DC) with an immunosuppressive phenotype.
A. Flow cytometry analysis of cell surface LILRB2 expression by IL-4 and IFN differentiated DC (black-filled histogram). Open histograms show staining with isotype control. Representative data from two individuals.
B. Flow cytometry histogram analyses of HLA-DR, CD86 and PD-L1 expression (black-filled histogram) by IFN-DC either untreated or treated with PBS or HLA-G2 as indicated. Open histograms show staining with isotype control. Representative data of three independent experiments from one individual.
C. IL-6 (left) and IL-10 (right) production by IFN-DCs with/without HLA-G2 (2.3 μM) treatment. Mean values with standard deviation from three independent experiments from one individual.

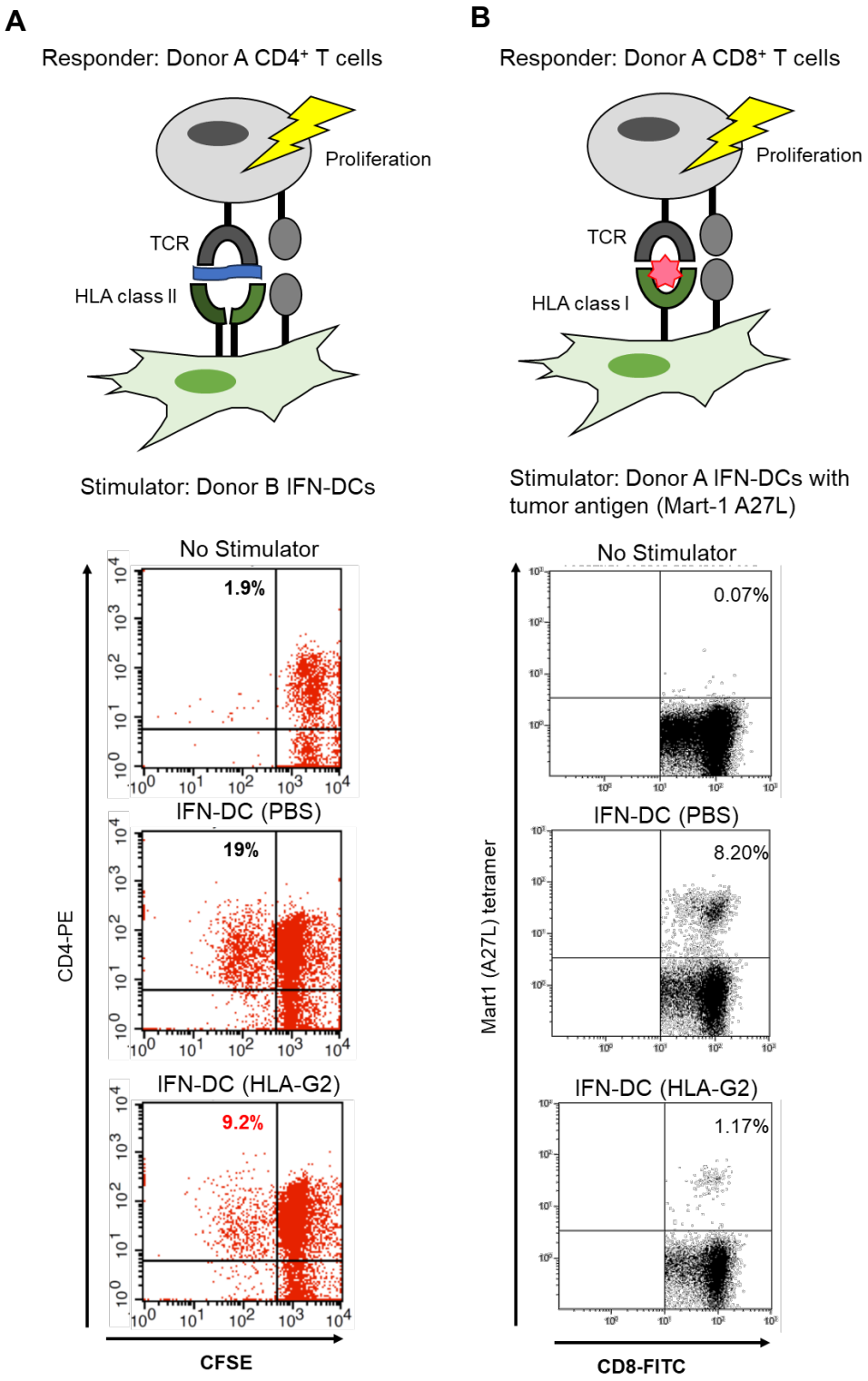

Figure 4. MLR of HLA-G2-treated IFN-DCs

A. Allogenic MLR analysis of CFSE-labelled T lymphocyte proliferation in response to IFN-DCs treated with or without HLA-G2 (2.3 μM) treatment. Dot plots show healthy donor $CD3^+$ T cell proliferation after six days culture with treated or untreated IFN-DC and IL-2 from a different healthy donor. The percentage of $CD4^+CD3^+$ T cells are shown in the left upper panels. Representative data from two independent experiments using two different healthy donor pairs are shown.

B. Autologous MLR analysis of CD8 T lymphocyte proliferation in response to culture with IL-2 and peptide-pulsed IFN-DCs from the same donor with or without HLA-G2 (2.3 μM) treatment. Dot blots show proliferation of CD8-positive T cells after 14-day stimulation. The percentage of CD8 positive T cells staining with MART-1 (A27L) tetramers cells are shown in the upper right quadrants. Plots show representative data from two independent experiments from one healthy HLA-A2-positive individual.

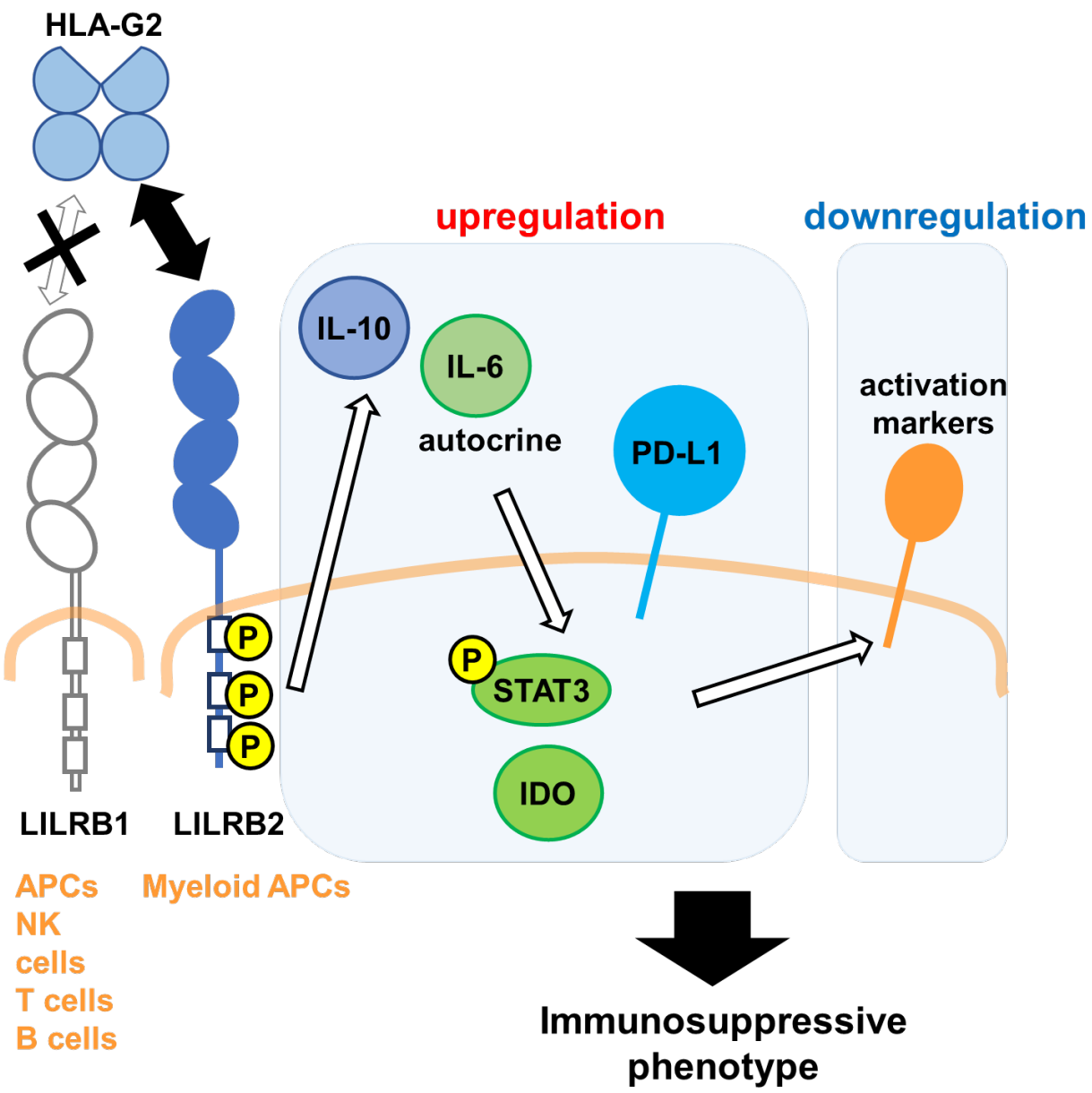

Figure 5. Model of the immunosuppressive mechanism of HLA-G2 in LILRB2-positive myelomonocytic cells